Non-destructive evaluation of the mechanical strength of a TA6V4/composite bond using LASA

In the current context of aircraft weight reduction and considering the trend for lowering production and maintenance costs, the aeronautics industry is promoting the use of adhesive bonds to replace mechanical fasteners. However, the main limitation of structural bonding in the aircraft industry is the ability to certify the good quality of a structural bond in a non-invasive way, i.e. to certify that the bond can resist up to a predefined strength value.

Simon Bardy, *CEA, DAM, DIF*
Mathieu Ducousso, *Safran Tech*
Tomas Bergara, *Rescoll*
Laurent Berthe, *Laboratoire Procédés et Ingénieries en Mécanique et Matériaux, CNRS, Arts et Métiers Paris Tech*
Laurent Videau, *CEA, DAM, DIF*
Frédéric Jenson, *Safran Tech*
Nicolas Cuvillier, *Safran Tech*

Conventional non-destructive testing (NDT) techniques (Ultrasonics, radiography, shearography,...) allow disbonding detection but are inefficient to evaluate the mechanical strength of bonds, i.e. detect weak bonds. A manufactured bonded part is not validated with 100% fiability with NDT technique. So, it is a huge lock for a wide use of bonding in structural bonding where maximal fiability is required. Thus, some industrials choose additionnal assemblying process to bonding such as bolding, riveting,...

Bonding is a compex process, divided into steps which has all to be fully-controled. Production defaults come from a lack of adhesion or a lack of adhesive cohesion due to various origins (pollution, micro-voids, uncomplete adhesive curing,...). Most of this defaults are nowadays not detected and detectable imposing a perfect bonding process control. That's why structural adhesives are hardly qualified in aeronautics. Laser Adhesion test opens a new way for NDT quantitative evaluationof bonded joints mechanical properties answering to industrial issue in bonding technology.

This process is based on the use of high energy laser which can genrate stresses localized in the bonding area.

The results presented were realized in the frame of Compochocproject which aims to develop an automatic device to perform LASAT inspection on industrial bonding.

The plateform which will be hosted by Rescoll in september 2018 and industrials will be able to perform NDT testing with LASAT process.

The LASer Adhesion Test (LASAT)[1] is seen as a promising alternative to traditional NDT techniques to reveal these weak bonds in a reproducible and automated way. This test consists in applying calibrated mechanical stresses to a given bonded assembly using laser-induced shock waves. This calibrated configuration should lead to disbonding of the joint/substrate interface in case of a weak bond while not damaging a healthy bond. Previous studies demonstrated the ability of the LASAT technology to characterize the quality of composite/composite bonded assemblies for typical operational thicknesses [2]. In the present work, LASAT is used to test two levels of adhesive bond mechanical strength for a TA6V4 titanium alloy/3D woven carbon/epoxy composite assembly. The potential of this technology for such a configuration is demonstrated as well.

LASAT principle

The LASAT technique is based on the following principle: a high-energy (E) pulsed laser beam is focused on some mm^2 of focal spot (S)

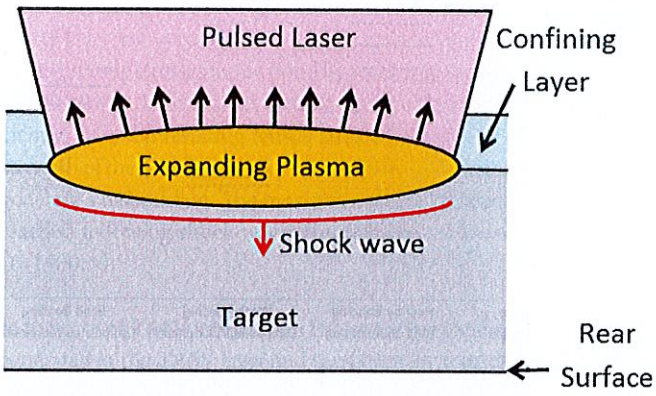

Fig. 1: Schematic view of the generation of a laser-induced shockwave in a confined geometry

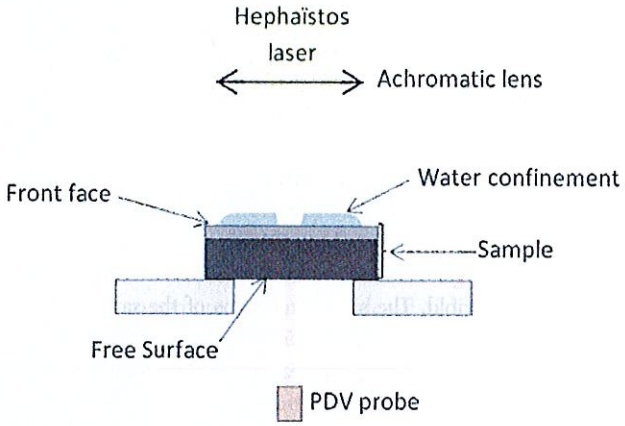

Fig. 2: Laser adhesion test configuration

on the front face of a given target for a time period (τ) of several nanoseconds. The laser pulse can therefore be characterized by its intensity (Equation 1).

$$I(GW/cm^2) = \frac{E(J)}{\tau(ns) * S(cm^2)}$$

Due to collisional absorption and inverse Bremsstrahlung phenomena [3], the matter is quickly heated up to the vapour and plasma state. According to Newton's third law, the ejection of matter from the front face towards the laser beam creates a reaction force in the opposite direction, i.e. towards the sample.

The use of a confining dielectric layer, such as water, has long been identified as an optimization technique to generate shocks with smaller laser intensities [4] (Figure 1). This type of geometry prevents plasma expansion and hence maximizes both the shock amplitude and duration. Nevertheless, it must be kept in mind that a water breakdown plasma occurs at intensities around 10 GW/cm², depending on the laser pulse duration and wavelength [5]. This phenomenon limits to a few GPa the maximum ablation pressure that can be applied to the target.

The amplitude (a few GPa) and duration (a few nanoseconds) of the resulting loading, named the ablation pressure (Pabl), imply strong temporal and spatial discontinuities, typical of a shock wave. The maximum ablation pressure can be estimated using well-known analytical laws [6] or even validated laser-matter interaction codes [7].

The shock wave generated in the front face then propagates through the thickness of the sample. According to acoustic impedance transmission-reflection laws, tensile stress zones can be generated due to the recombination of release waves. If the applied tensile stress is higher than the dynamic mechanical resistance of the bond, then a cohesive or adhesive fracture of the bond is observed. However, the use of conventional NDT techniques for the post-shock evaluation is necessary to determine which laser shots lead to disbonding. The LASAT technique coupled with a disbonding diagnostic can therefore be seen as a proof test since the use of a calibrated laser pulse should discriminate weak bonds from healthy ones. The main challenge for industrial applications is to demonstrate the non-destructive side of LASAT. This work brings some serious results assessing the NDT capacity of the technique.

Experiments

Materials

The samples investigated are made of a TA6V titanium alloy/3D woven composite bonded together with a typical aeronautic epoxy glue. The thickness of the titanium, glue and composite is 0.4 mm, 0.150 mm and 3.8 mm, respectively, for the considered samples. The side dimensions of the bonding are 240x40 mm².

Two different mechanical grades of bonding quality were achieved varying the glue reticulation during the curing step. The mechanical properties of the resulting bond quality were investigated using typical static mechanical testing methods. The results are shown in Table 1.

Tab. 1: Mechanical strength of the samples

	Healthy bond	Weak bond
Shear mechanical strength	35 MPa	15 MPa
Longitudinal mechanical strength	39 MPa	10 MPa

As expected, the healthy bond has a higher failure resistance than the weak bond. Weak-to- healthy properties were expected to be about 50%. The results differ significantly depending on the mechanical stress.

Laser facility

LASAT experiments were performed in the Hephaistos facility at the ENSAM-Paris PIMM (Procédés et Ingénierie en Mécanique et Matériaux) laboratory. This installation can produce 7-ns FWHM Gaussian pulses in the visible wavelength spectrum (532 nm). This Thales Gaia HP laser can generate up to 14 J that can be deposited on the target in a single pulse.

In the experiments, the Hephaistos laser beam was focused on the front face of the material, either the TA6V4 or the 3D composite face (Figure 2). A water-confined regime was used to maximize the applied

pressure. Back-face velocity monitoring was achieved using a PDV system [8] to follow the main back and forth travels of shock waves within the thickness of the sample.

Procedure

The disbonding thresholds were investigated for both types of mechanical strength. Using two samples for each mechanical grade also made it possible to investigate both TA6V and composite front-face configurations, i.e. to see how the impacted face could influence the disbonding threshold. The side dimensions of the samples enabled about 10 laser shots per sample (Figure 3). With this distribution, there were about 20mm between each laser spot, ensuring that the shots did not influence one another. A 6mm focal spot diameter was used to maximize the size of the induced disbondings, and hence their detectability. With this geometry, intensities just beyond the water breakdown threshold could be reached (see Equation 1), thus maximizing the ablation pressures used. In addition, the diameter-to-thickness ratio of the focal spot stayed relatively high, ensuring 1D shock propagation. In each bonding quality/front face configuration, gradual intensities were applied from 0.5 to 6 GW/cm².

After the LASAT experiments, an ultrasonic inspection in water immersion with transmission configuration was used to detect laser-induced disbonding. An emitting transducer worked at 15 MHz and reception was achieved with the help of a 10 MHz sensor.

Results

Disbonding thresholds

The laser shots for each configuration are referenced in Figure 4 with the corresponding intensity and ultrasonic (US) evaluation of the bond state. The disbonding thresholds are provided in Table 2. The threshold uncertainty is considered to be only impacted by the laser energy uncertainty, which is about 10%.

First, it was noticed that whatever the illumination side, the disbonding thresholds are clearly different for healthy bonds and weak bonds. This shows the potential of the LASAT technique to identify weak bonds by applying a calibrated laser pulse, above the weak bond threshold and beyond the nominal bond threshold. For example, illuminating such a sample with a 4GW/cm² pulse on the TA6V side will

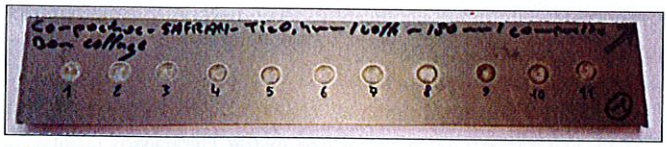

Fig. 3: Front face of a TA6V/composite sample after laser ablation

Tab. 2: Disbonding thresholds identified by US inspection after LASAT

	TA6V illumination	Composite illumination
Healthy bond	5.2 GW/cm² (+/- 0.5 GW/cm²)	4.25 GW/cm² (+/- 0.4 GW/cm²)
Weak bond	3.25 GW/cm² (+/- 0.3 GW/cm²)	2.25 GW/cm² (+/- 0.2 GW/cm²)

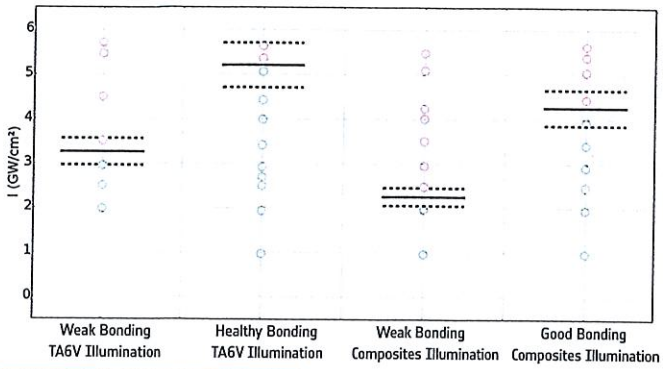

Fig. 4: Summary of laser shots for each configuration with US disbonding diagnostic (green circles – no disbonding detected, red circles – disbonding detected) and disbonding thresholds as black lines (threshold uncertainty is shown with dotted lines)

leave a healthy bond intact and induce a disbonding in a weak bond. Post-shock US scanning would reveal a possible disbonding and hence determine if the sample is a healthy bond or not.

A slight difference was seen whether the shock was generated on the TA6V side or on the composite side. This difference was most probably due to different wave propagation patterns within the samples.

Time-position diagrams

At the same time, numerical simulations were realized in order to better understand phenomena during LASAT tests aiming to be able to predict bonding mechanical behaviour and to optimize experimental parameters (intensity, pulse time, pulse form, spot diameter,...).

Simulations were conducted using a 1D-hydrodynamic code with simple material models. These simulations produce the time-position (X-t) diagram corresponding to 3GW/cm² experiments. The same laser loading (ablation pressure) is applied at t=X=0 for both configurations: TA6V illumination and composite illumination. Tensile stresses in the joint appear at different times, depending on the type of configuration used, in relation with an impedance mismatch in the three layers (ZEpoxy = 3.106 Pa.s-1, ZComposite = 5.106 Pa.s-1 and ZTA6V = 15.106 Pa.s-1).

In the case of composite irradiation (Figure 5), the incident shock waves travelling in the composite interact with the composite/epoxy interface (X=-3.8mm). Due to relatively close acoustic impedances on each side of this interface, the amplitude of the reflected release wave (ZComposite>ZEpoxy) is rather small and most of the incident energy is transmitted as a shock wave in the epoxy layer. The resulting wave transmitted in the epoxy layer is a shock wave that then interacts with the epoxy/TA6V interface (X=-3.95mm). The reflected wave is a shock wave (ZEpoxy < ZTA6V) going backward in the epoxy layer and then in the composite. The wave transmitted at this interface is a shock wave propagating in the TA6V, which will then reflect itself as a release wave at the free surface on the back face of the material (X=- 4.35mm – t=1100 ns). This release wave is partially reflected as a shock wave at the TA6V/epoxy interface as it goes backward and a corresponding transmitted release wave goes back in the epoxy layer and then in the composite. Quick back and forth travels of the shock waves trapped within the TA6V layer can be seen due to the high impedance mismatch between the TA6V and the epoxy.

This propagation pattern generates successive release waves in the epoxy layer between 1100 and 2000 nanoseconds, progressively inducing tensile stresses in the bond by recombination with the incident release waves. If the initial loading (laser ablation pressure) is sufficiently high, the resulting tensile stresses can exceed the mechanical strength of the bond and/or the composite/epoxy interface and hence generate a disbonding. The maximum tensile stresses in the bond are reached following shock waves through the thickness of the sample (t=1500ns).

In the case of TA6V irradiation (Figure 6), the incident shock wave is generated in the TA6V layer and then partially transmitted as a shock wave at the TA6V/epoxy interface (X=-0.4mm). The wave reflected at this interface is a release wave (ZTA6V > ZEpoxy) that goes back to the front face and reflects again as a shock wave in the TA6V layer. The shock wave pattern in the TA6V layer is very comparable to the one exposed in the composite illumination configuration, except that it generates successive shock waves in the rest of the sample. These shock waves travel in the epoxy layer and are transmitted in the composite as a shock wave. The reflection of these shock waves at the epoxy/composite interface (X=-0.55mm) is neglected here due to their low amplitude. The first incident shock wave in the composite reaches the composite free surface of the sample (X=-4.35mm – t=1100ns), where it is fully reflected as a release wave. The recombination of this reflected release wave with incident ones creates a tensile stress zone. This tensile zone then goes backward and reaches the epoxy layer. As described before, disbonding occurs if the maximum tensile stresses exceed the mechanical strength of the bond and/or the composite/epoxy interface.

However, in this case, the shock waves propagate twice through the composite before generating maximum tensile stresses at the interface (t=2500 ns).

The shock wave propagation patterns shown here suggest that the composite illumination side is an optimum configuration for LASAT. Shock waves propagate on a shorter acoustic path in that configuration and, hence, are less subjected to attenuation through the composite. This is believed to account for the dependence of disbonding thresholds on the illumination side. However, 2D or 3D simulations with a developed composite model, taking anisotropy into account, are required. This should enable a quantitative simulation of shockwave attenuation and thus provide a more precise stress evaluation within the stacking. A quantitative evaluation of the bond mechanical strength would be possible with the set of experimental data exposed here.

Free surface velocity measurement

Free surface velocities (FSV) on the back face of the sample also showed some interesting results. In the configurations with laser illumination on the composite side, a strong correlation between FSVs and ultrasonic diagnostics can be identified.

In fact, the FSVs recorded during the experiments leading to bond failure exhibit a spallation- type curve [9] [10]. In Figure 7, for example, the laser shot achieved at 0.97GW/cm² (black curve) shows a clear back and forth travel of shock waves in the whole stacking. FSV oscillates around 0 m/s. A negative FSV might be induced by two-di-

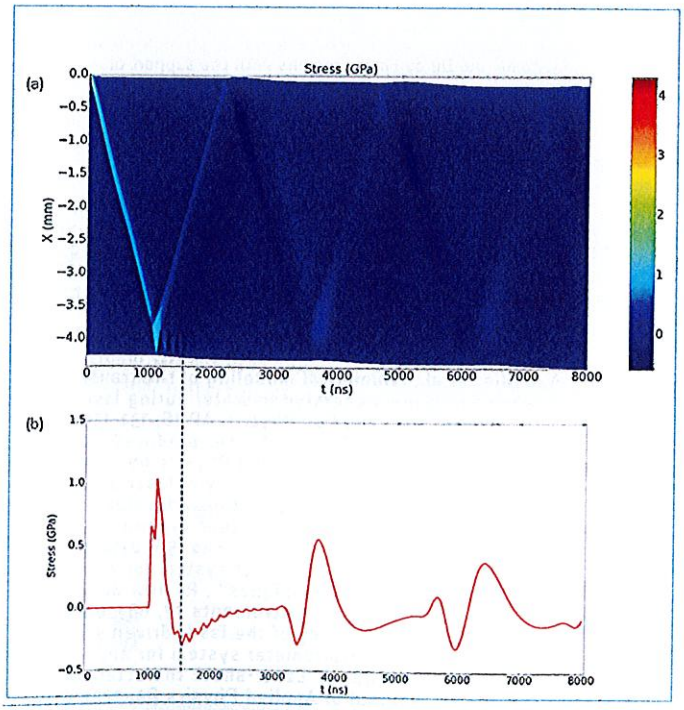

Fig. 5: (a) Time-position (X-t) stress diagram; and (b) stress evolution at the epoxy/composite interface in the composite illumination case

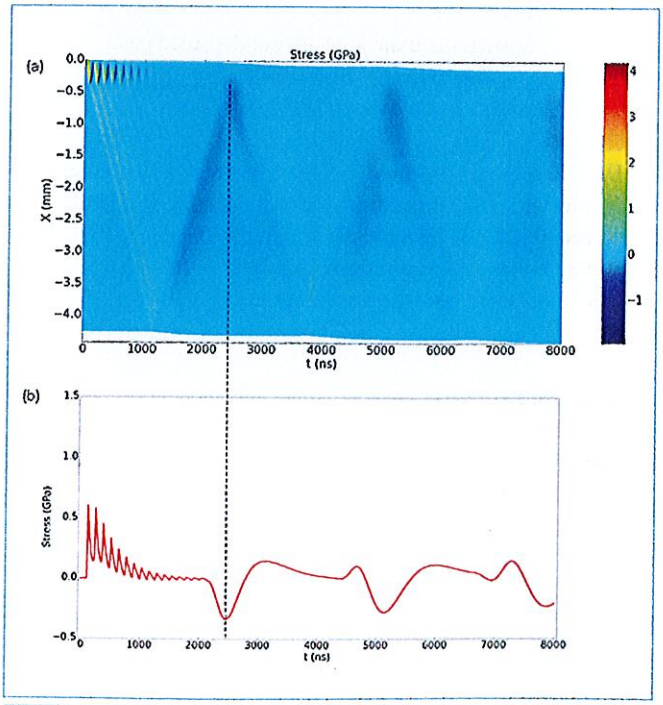

Fig. 6: (a) Time-position (X-t) stress diagram; and (b) stress evolution at the epoxy/composite interface in the TA6V illumination case

mensional effects. The corresponding period for this type of event is about 3 µs, which is coherent with the longitudinal shock velocity of the constitutive materials. Conversely, disbonding implies the creation of a free surface at the TA6V/epoxy interface, meaning this layer is not unloaded by release waves like the rest of the sample and, therefore, its FSV profile exhibits a quasi-constant velocity just after the main peak. Back and forth travels of the shock waves in the TA6V layer will generate FSV oscillations after disbonding (Figure 5 (a)). However, the temporal resolution of the PDV analysis used here (50 ns) will prevent these oscillations from being detected. It also seems that FSV curves might be impacted by two-dimensional effects as negative values are visible in some cases. These edge effects are hardly understandable without an appropriate simulation.

Non-destructive testing

Finally, post-shock micrographs of the samples subjected to the highest intensities did not reveal any failure in the composite or the TA6V layer.

A separate characterization of the TA6V and the 3D composite layer under laser shock in the same conditions (thickness and laser intensity) had already resulted in the same observation.
These observations show that in this case, laser-induced shocks do not seem to have affected the material. The LASAT configuration used here does not seem to induce damage in the substrates. Regarding the nature of the substrates and the respective thickness of the materials, it seems that the LASAT configurations used in this study are non-destructive.

Deeper investigations are required to assess LASAT as a non-destructive method. Mechanical testing after laser shocks is planned to confirm that the substrates and the joint are not degraded below their respective damaging threshold.

Conclusion

The LASAT configuration used can discriminate a weak bond from a healthy one with the help of disbonding diagnostics. In addition, the healthy bond's disbonding threshold was clearly identified. This means that a weak bond just beyond the tolerance (+/- 20% of the healthy strength) should also be discriminated using the same configuration. Some further experiments should be conducted with such a bond quality.
In-situ free surface velocimetry provided encouraging results for detecting disbonding in a given configuration. Deeper investigations are necessary to confirm this technique's potential to detect disbonding coupled with laser-induced shock waves.

Post-shock diagnostics confirmed the potential of LASAT as a non-destructive method. However, some modifications of the material due to the shock might be non-detectable, even with micrographs. Mechanical testing of samples subjected to laser shocks is necessary to demonstrate the non-destructive nature of such a technology.
1D simulation was used to build the time-position diagrams required to understand the shock wave propagation patterns involved. Based on these tools, an interpretation of the disbonding threshold dependence on the illumination side was proposed.
2D or 3D simulations are needed to simulate attenuation phenomena and edge effects more precisely. A quantitative simulation could provide more information on the evolution of stresses within the substrates and, if needed, help to define a more optimized configuration to lower stresses in the substrates, while still covering weak bond detection. In addition, the mechanical resistance of bonds under shock loading could be determined using such a simulation. □

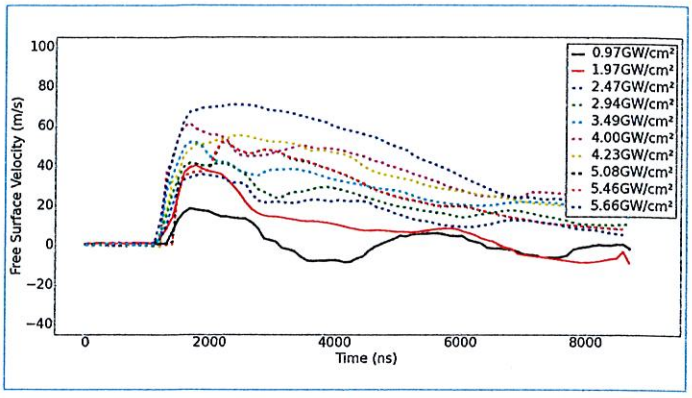

Fig. 7: Evolution of the free surface velocity with time for composite illumination shots on a weak bond - Temporal resolution = 50 ns - Signals in dotted lines correspond to identified disbonding configurations

More information:
Ducousso Mathieu (Safran), mathieu.ducousso@safrangroup.com
Bergara Tomas (Rescoll), tomas.bergara@rescoll.fr

Acknowledgement
The authors would like to acknowledge the consortium of the Compochoc project composed by the following companies: Alphanol, Airbus, CEA, Cilas, Idil, Kuka Aerospace,Laser Metrologie, PIMM, PSA Peugeot Citroen, Rescoll, Safran, Simchoc. This project received funding from the FUI french program and Nouvelle-Aquitaine and Ile de France regions with the support of Aerospace Valley, Astech and Route des Lasers.

References

[1]. L. Berthe et al., "State-of-the-art laser adhesion test (LASAT)," Nondestructive Testing and Evaluation, 26 (3-4), 303-317 (2011)
[2]. R. Ecault et al., "Development of a laser shock wave adhesion test for the detection of weak composite bonds," 5th International Symposium on NDT in Aerospace, Singapore (2013)
[3]. P. Mora, "Theoretical model of absorption of laser light by a plasma," Phys. Fluids 25, 1051 (1982)
[4]. N. C. Anderholm, "Laser-generated stress waves," Appl. Phys. Lett. 16, 113 (1970)
[5]. A. Sollier et al., "Numerical modeling of the transmission of breakdown plasma generated in water during laser shock processing," The Eur. Phys. J. AP 16, 131-139 (2001)
[6]. R. Fabbro, "Physical study of laser-produced plasma in confined geometry", Journal of Applied Physics 68, 775 (1990)
[7]. S. Bardy et al., "Numerical study of laser ablation on aluminum for shock-wave applications: development of a suitable model by comparison with recent experiments", Opt. Eng. 56, 011014 (2016)
[8]. O. T. Strand et al., "Compact system for high-speed velocimetry using heterodyne techniques" , Review of Scientific Instruments 77, 083108 (2006)
[9]. L. Tollier et al., "Study of the laser-driven spallation process by the velocity interferometer system for any reflector interferometry technique. I. Laser-shock characterization.", Journal of Applied Physics 83, 1224 (1998)
[10]. L. Tollier et al., "Study of the laser-driven spallation process by the VISAR interferometry technique. II. Experiment and simulation of the spallation process.", Journal of Applied Physics 83, 1224 (1998)